https://doi.org/10.31436/iiumej.v25i2.3250

DESIGN AND DEVELOPMENT OF A SLIDER-CRANK ACTUATED KNEE EXOSKELETON WITH OPTIMIZED MOTION CONTROLLER

MARIAM MD GHAZALY[1,2]*, NAI JUN AN[1,2], LAW HIN KWEE[1,2], ZULKEFLEE ABDULLAH[3], NORHASLINDA HASIM[1,2], ISA HALIM[3], NASHARUDDIN ZAINAL[4]

[1]*Motion Control Research Laboratory (MCon Lab), Fakulti Teknologi dan Kejuruteraan Elektrik (FTKE), Universiti Teknikal Malaysia Melaka, Melaka, Malaysia*
[2]*Center for Robotics and Industrial Automation (CeRIA), Universiti Teknikal Malaysia Melaka, Universiti Teknikal Malaysia Melaka, Melaka, Malaysia*
[3]*Fakulti Teknologi dan Kejuruteraan Industri dan Pembuatan (FTKIP), Universiti Teknikal Malaysia Melaka, Melaka, Malaysia*
[4]*Department of Electrical, Electronic, and Systems Engineering, Faculty of Engineering and Built Environment, Universiti Kebangsaan Malaysia, Bangi, Malaysia*

**Corresponding author: mariam@utem.edu.my*

(Received: 4 April 2024; Accepted: 27 June 2024; Published online: 15 July 2024)

ABSTRACT: The rising incidence of injuries and neurological disorders has highlighted the critical need for accessible and affordable rehabilitation solutions. In response to this demand, robotic exoskeletons have become a popular option for rehabilitation. However, current rehabilitation exoskeletons are generally expensive due to the high force of the actuators used, i.e., electric motors. Therefore, the availability is limited to patients who can afford to pay for physiotherapy using these robotic exoskeletons. Because of the demand for high force, the exoskeleton is heavy, impacting patient safety. In response to these challenges, the main contribution of this study is to develop a lightweight lower-body rehabilitation exoskeleton with sufficient force while maintaining a fast response time and precise motion control for rehabilitation purposes. In this research, a lower body knee joint rehabilitation exoskeleton prototype implementing a slider-crank mechanism was meticulously designed and optimized using Finite Element Analysis (FEA) via SolidWorks software. After optimising the design, the lower body exoskeleton (LBE) was fabricated and assembled. Next, the LBE system was characterized to understand its non-linear behaviour, as the LBE uses a double-acting pneumatic cylinder that is known to exhibit non-linear behaviour. To further analyse the effectiveness of LBE for rehabilitation, a Proportional-Integral-Derivative (PID) controller was adopted for its simplicity in controlling the exoskeleton's angular motions. Excellent results were obtained using a PID controller at the angular displacement of 75^{o}, with a 96.5% reduction in overshoot (OS%), a 92.9% decrease in steady-state error (E_{ss}), a 3.2% reduction of rise time (T_r), and a minimal 0.006% reduction in settling time (T_s). These findings indicate that the LBE with the slider-crank mechanism is a promising device, particularly for knee joint rehabilitation, and that it can be applied to other rehabilitation applications that require a lightweight design and high force application.

ABSTRAK: Peningkatan kecederaan dan gangguan neurologi menyebabkan keperluan kritikal terhadap pemulihan yang senang diakses dan berpatutan. Sebagai solusi kepada keperluan ini, robot eksoskleton telah menjadi pilihan popular bagi sesi pemulihan. Namun, eksoskleton pemulihan sedia ada adalah secara amnya mahal kerana memerlukan daya

penggerak yang tinggi, contohnya motor elektrik. Maka, ketersediaan menggunakan eksoskleton pemulihan ini terhad kepada pesakit yang mampu membayar fisioterapi mahal menggunakan robot eksoskleton. Selain itu, disebabkan permintaan pada daya penggerak tinggi, robot eksoskleton secara tidak langsung adalah berat dan ini akan memberi kesan kepada keselamatan pesakit. Sebagai solusi kepada permasalahan ini, sumbangan utama kajian ini adalah bagi membangunkan eksoskleton pemulihan bahagian bawah badan yang ringan dan mempunyai daya penggerak yang mencukupi, di samping mengekalkan masa tindak balas yang cepat dan kawalan pergerakan yang tepat bagi tujuan pemulihan. Penyelidikan ini membangunkan prototaip eksoskleton pemulihan sendi lutut bawah badan (LBE) yang menggunakan mekanisme engkol gelangsar dan dioptimumkan dengan teliti menggunakan Analisis Unsur Terhingga (FEA), menggunakan perisian SolidWorks. Selepas reka bentuk dioptimumkan, eksoskleton LBE telah difabrikasi dan dipasang. Seterusnya sistem LBE telah direka bagi memahami ciri-ciri tidak linear, kerana sistem LBE ini menggunakan silinder pneumatik dwitindakan, dimana pneumatik terkenal sebagai sistem tidak linear. Bagi menganalisa lebih lanjut keberkesanan LBE sebagai sistem pemulihan, kawalan Berkadaran-Kamiran-Pembeza (PID) telah digunakan bagi memudahkan kawalan sudut gerakan eksoskleton. Dapatan kajian menunjukkan, kawalan PID adalah sangat baik pada gerakan sudut maksimum, anjakan sudut 75^{o}, di mana pengurangan 96.5% yang ketara dalam lajakan (OS%), penurunan 92.9% dalam ralat keadaan mantap (E_{ss}), 3.2% pengurangan masa naik (T_r), dan pengurangan minimum 0.006% dalam masa penetapan (T_s). Penemuan ini menunjukkan bahawa sistem LBE dengan menggunakan mekanisme engkol gelangsar adalah peralatan yang berkesan, terutama bagi pemulihan sendi lutut, dan ia juga boleh digunakan bagi aplikasi pemulihan lain yang memerlukan reka bentuk ringan dan aplikasi daya yang tinggi.

KEYWORDS: *Lower Body Exoskeleton (LBE), Knee Joint Rehabilitation, Slider-Crank, Finite Element Analysis (FEA), PID controller.*

1. INTRODUCTION

Exoskeletons are versatile external wearable devices with a wide range of applications. They are useful tools for specific tasks, daily activities, and medical rehabilitation, particularly for people who have mobility impairments as a result of spinal cord injuries, stroke, or traumatic events [1-6]. Figure 1 depicts examples of a lower body exoskeleton (LBE), BLEEX (Berkeley Lower Extremity Exoskeleton), designed by the University of California, Berkeley, in 2000. BLEEX was the first autonomous robotic exoskeleton demonstrated to allow the user to carry significant loads over various terrains [7,8]. In contrast, Hybrid Assistive Leg (HAL) is used for walking gait training, whilst Lokomat and ReWalk are used for walking rehabilitation therapy [10-12]. These advanced exoskeletons not only greatly assist in the rehabilitation of stroke patients and the well-being of the elderly, but they can also reduce physical strain in industries such as construction, manufacturing, and logistics [13-17]. In Figure 1, HAL-ML05 refers to the Hybrid Assistive Leg, model ML05, which is used as a medical device for patients suffering from musculoskeletal ambulation disability symptom complex, which includes spinal cord injuries, traumatic brain injuries, cerebrovascular diseases, and other brain and neuromuscular disorders.

https://doi.org/10.31436/iiumej.v25i2.3250

(a) BLEEX [7] HAL-ML05 [9]

Figure 1. Examples of a lower body exoskeleton (LBE)

Nevertheless, the adoption of lower body exoskeletons (LBE) is hampered by limitations such as high costs and complex controllers, making them unfeasible in some regions despite their improved functionality [18,19]. Simplified control systems are required for effective user mobility. Moreover, problems such as the weight of the exoskeletons, low torque, and risk of falls to patients with existing exoskeletons are some of the challenges that need to be considered [20-22]. In response, researchers are working on designing LBE with higher torque and power for lower-body applications using advanced materials and control algorithms [23]. They are also trying to enhance the precision and the rate of the intention-detecting sensors by integrating advanced sensor technologies with machine learning techniques like EMG and motion capture [5,20,21,24,25]. Large-size machine-type supported exoskeletons offer mechanical aid for patients with full disability; however, they are often too bulky, expensive, and too sophisticated for use in hospitals [26-28]. Mobile exoskeletons are lighter and more portable but have drawbacks like shorter battery life and no back support, which restricts the duration of use [11, 29-31]. Moreover, fixed exoskeletons, which are intended for the treadmill, are rather bulky, costly, and possess low mobility [32,33]. Therefore, the aim of this research is to design a lower body rehabilitation exoskeleton that is lightweight and has enough force to support the patient's body weight during rehabilitation while at the same time having a fast response time and accurate control of the motion.

Exoskeletons employ different types of actuators, such as pneumatic, hydraulic, and electrical systems, with their own advantages and disadvantages. For instance, pneumatic actuators can offer linear motion and high-speed benefits with some designs, but they may not be as accurate and may be affected by issues like non-linear airflow and air leakage [34-36]. Hydraulic actuators, for instance, in BLEEX, offer accurate control because the hydraulic fluid is incompressible, but they are known to leak and cause-related injuries [7,8,37]. Electrical actuators employ brushed DC motors for high accuracy; however, they are costly compared to other types [38,39]. In addition, exoskeletons also employ several mechanisms for motion conversion. The slider-crank mechanism is widely used and is a type of kinematic pair that translates rotational motion into linear motion to help in joint

movement, especially in the knee and elbow joints; it offers simplicity and high rigidity within a small range of motion with an added bonus of being lightweight [40-41]. The rack and pinion system that translates rotary motion to linear motion is employed in exoskeletons due to its compactness and high torque density, but it is relatively large and thus may not be portable [42]. Ball screw mechanisms are also used, which are efficient and precise, but they produce high heat and are quite bulky [43].

For proper movement of the exoskeleton, appropriate controller techniques are needed. Traditional approaches like the PID controller use feedback control algorithms to achieve the desired motion while being easy to design [44-47]. Tuning of a PID controller is crucial in order to get the desired performance of a system and this can be done in several ways, each of which has its own benefits. Heuristic methods such as the Trial-and-error method, Ziegler-Nichols, and Cohen-Coon are some of the systematic tuning methods that use system responses to give initial settings for further fine-tuning. The trial-and-error method is a simple method of adjusting the system based on the response of the system, which is easy to implement and gives an immediate response to the system, hence making it effective despite its simplicity. Root locus, bode plot, and Nyquist plot are other methods that provide graphical solutions for stability and performance analysis, which are more complex and need more control theory knowledge. Genetic algorithms, particle swarm optimization, and simulated annealing are some of the computational methods that employ sophisticated techniques to search for the best parameter space and optimize PID gains for complicated systems, but they are time-consuming. Model-based optimization techniques such as Linear Quadratic Regulator (LQR) and Model Predictive Control (MPC) employ state-space models and predictive algorithms to determine the best control actions, offering high accuracy in exchange for accurate system models and high computational demands. Each method is useful, and the choice depends on the application needs and the system's characteristics, which enables the best approach to achieve the best performance of the controller and the system's stability. On the other hand, Artificial Intelligence (AI) based controller strategies, such as machine learning and model-based control, can enhance flexibility and accuracy at the cost of high computational complexity. In addition, a mixed approach integrates machine learning and model-based control, which brings complexity but also flexibility and accuracy [48,49]. Position-based trajectory tracking control involves following joint paths and while it has its drawbacks, it is not easy to model dynamics [50]. Some exoskeletons rely on electromyographic (EMG) signals to control the motion intent and patient recovery status, using methods like stiffness regulation and joint position with EMG information [51-56].

In conclusion, this research aims to develop a lightweight lower body exoskeleton (LBE) movement using a slider-crank mechanism coupled with a double-acting pneumatic actuator to overcome the limitations of current exoskeletons for knee joint rehabilitation in a seated position, using conventional control strategies, that is, a PID controller due to its simplicity, reliability, and flexibility. The slider-crank mechanism and pneumatic actuators are more preferred than other mechanisms and actuation systems, which makes the design lightweight, user-friendly, and safe for patients who are undergoing rehabilitation. The slider-crank mechanism translates rotational motion into linear movement, thus making joint motion simpler, stronger, and more effective, especially in the knee joints. Pneumatic actuators are particularly suitable for linear motion, speed, and force, which makes them suitable for applications that require fast and accurate control of motion.

https://doi.org/10.31436/iiumej.v25i2.3250

2. METHODOLOGY

This section presents the design of the lower body exoskeleton (LBE) prototype using SolidWorks software, the optimization of the LBE design using Finite Element Analysis (FEA), and the discussion on the LBE full experimental setup. To validate the LBE prototype, the LBE was characterized in order to gain insight into the system's non-linear response. After the LBE was characterized, the PID controller was designed using a heuristic approach because of its ability to handle non-linear systems such as the LBE system.

2.1 Lower Body Exoskeleton (LBE) Experiment Setup

This research focuses on the design of a lower-body exoskeleton (LBE) prototype with the aim of knee joint rehabilitation using a slider-crank mechanism in a seated position. To ensure that the exoskeleton device is practical for use, the LBE was designed with the human anatomy specification in mind. It is vital that the device does not restrict the user's movement and allows for safe movement. The biomechanical properties of the body need to be considered, including the location of joints, limb length, limb weight, and the maximum range of motion at the knee joint. This information is necessary to design a device compatible with the patient's body [57,58]. Therefore, the working range for the LBE is set to between 0° to 75°. The knee possesses two rotational degrees of freedom and is classified as a condyloid joint; however, it is frequently reduced to a one DOF joint since the twisting rotation of the joint is restricted and not always necessary for movement. Figure 2 shows the overview of the LBE prototype, which was meticulously designed using SolidWorks. The individual components were designed separately, optimized, and assembled. The LBE consists of two (2) double-acting pneumatic cylinders, pusher holders, leg holders, piston end pins, knee rods, cranks, shank holders, and sliders, with plywood as the frame material. The Finite Element Analysis (FEA) method was employed to comprehensively assess the LBE structural integrity and performance under varying conditions and loads, as illustrated in Figure 3. The FEA analysis was conducted on four crucial LBE components, i.e., Shank 1, Shank 2 (plywood with yield strength 13.8×10^6 N/m^{2}Pa), Pusher Holder (Aluminum 7075 with yield strength 480×10^6 N/m^2), and Slider.

Based on Figure 3, the FEA analysis aims to assess the stress distribution and the safety factor, contributing to a comprehensive understanding of the prototype's performance and durability. The red-colored area in the Finite Element Analysis (FEA) result indicates the areas of high-stress concentration in Shank 2 of the LBE design. The FEA result for Shank 2 suggests that this component experienced significant stress when the load was applied to it, which is crucial information for assessing the structural integrity and performance of the LBE prototype under varying conditions and loads. Table 1 summarizes the FEA results for each component. Based on the analysis, the FEA confirms that the component can withstand applied forces of up to 367 N, which represents the total force exerted by two (2) double-acting pneumatic cylinders, which is still within its yield strength limits, and ensuring resilience against deformation or failure. Furthermore, the factor of safety analysis affirms that all materials used have a factor of safety exceeding one, signifying their capacity to withstand applied forces without damage.

Based on the FEA results, the LBE prototype was fabricated. Figure 4 shows the LBE overall experiment setup comprised of the LBE prototype, which is connected with the OMRON Rotary Encoder (E6B2CWZ6C). The encoder acts as the feedback to the LBE system, which is used for angular motion control. Two (2) double-acting cylinders (Chelic SDA 20/075) convert the LBE linear motion to angular motion using the slider-crank mechanism shown in Figure 2. To control the double-acting cylinders, the Enfield

https://doi.org/10.31436/iiumej.v25i2.3250

Technologies 5/3 Proportional Directional Valve (LS-V05S) was implemented to control the linear bi-directional motion, hence converting the linear motion to rotary motion via the slider-crank mechanism. For the purpose of controlling the pressure input to the LBE system, two (2) pressure sensors, FESTO SDE3-D10S-B-HQ4-2P-M8, were mounted on the LBE system. To evaluate the control performances of the LBE system, MATLAB/ SIMULINK was implemented and was connected in real-time via a DSP board, i.e., Micro-Box 2000/2000C for the real-time control system.

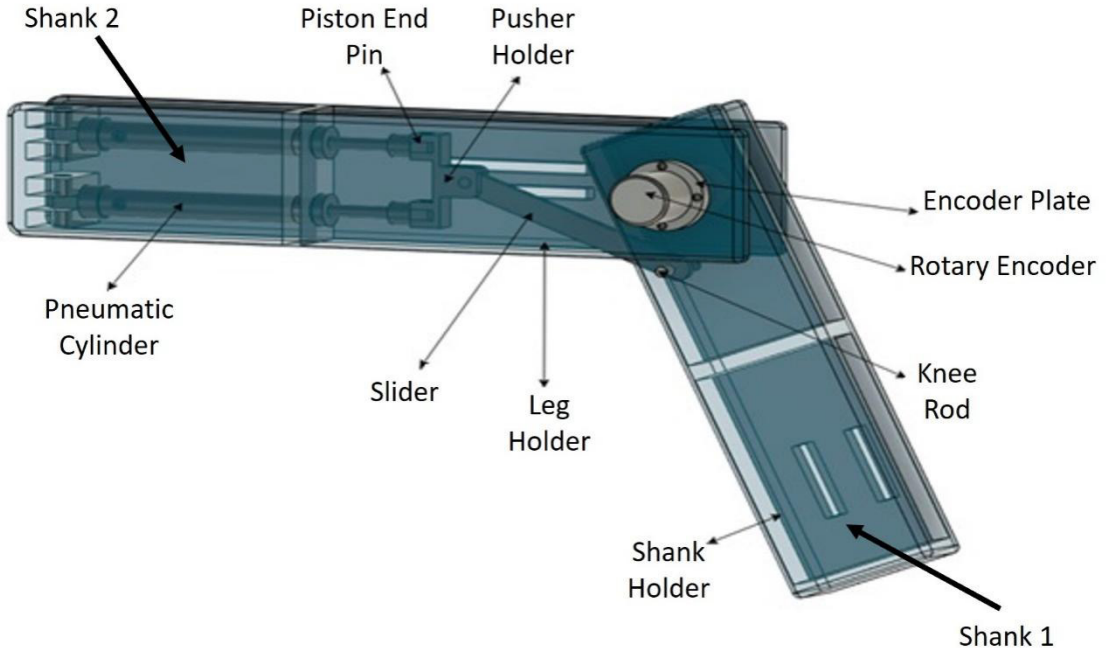

Figure 2. Design overview of the LBE system

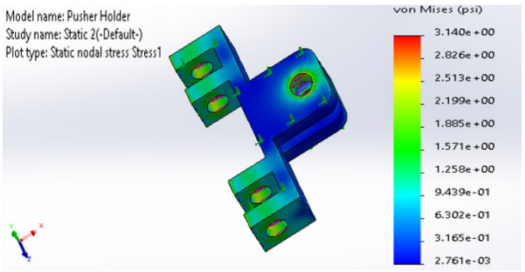

(a) Push Holder Stress Analysis

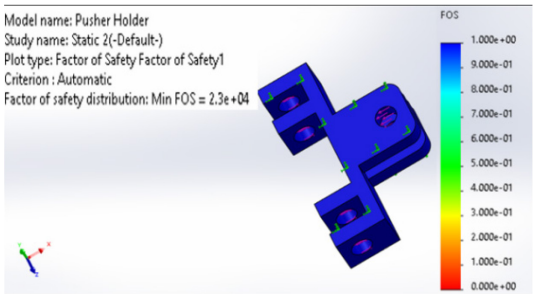

(b) Push Holder Factor of Safety Analysis

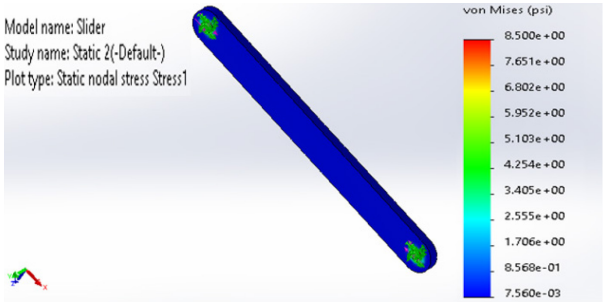

(c) Slider Stress Analysis

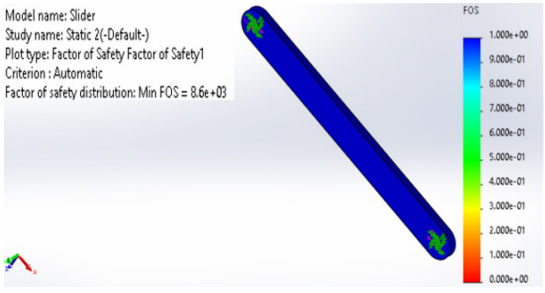

(d) Slider Factor of Safety Analysis

https://doi.org/10.31436/iiumej.v25i2.3250

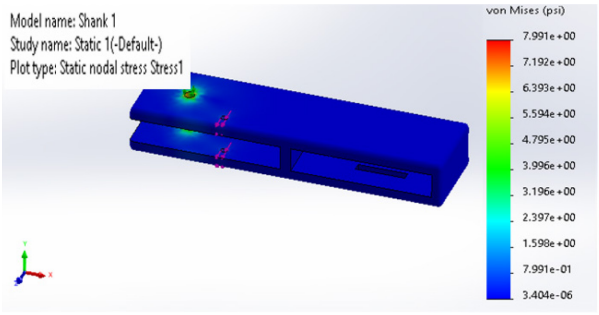

(e) Shank 1 Stress Analysis

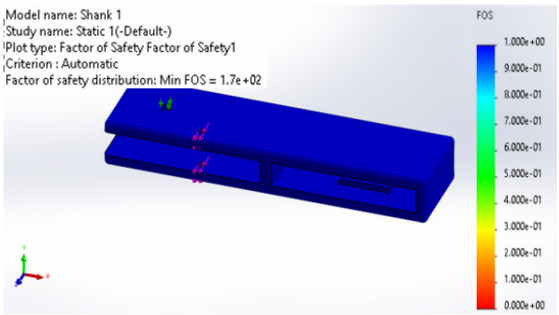

(f) Shank 1 Factor of Safety Analysis

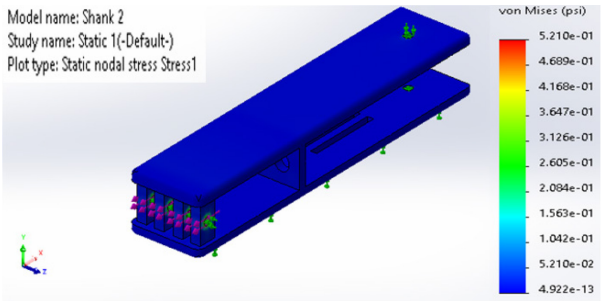

(g) Shank 2 Stress Analysis

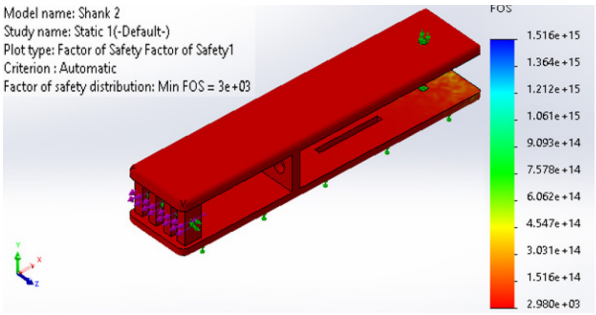

(h) Shank 2 Factor of Safety Analysis

Figure 3. Finite Element Analysis (FEA) results for the LBE components.

Table 1. FEA test result data

Component part Test	Stress Limit	Strain Limit	Static Displacement Limit	Factor of Safety	Component part Test
Pusher Holder	21649.54 (N/m2)	6.649e-8	6.284e-6 mm	2.3 ×104, >1	Pusher Holder
Slider	58605.4 (N/m2)	10.991e-8	3.549e-7 mm	8.6 ×103, >1	Slider
Shank 1	55096.01 (N/m2)	6.634e-6	3.142e-1 mm	1.7 ×10, >1	Shank 1
Shank 2	3592.17 (N/m2)	4.612e-7	3.965e-6 mm	3 ×103, >1	Shank 2

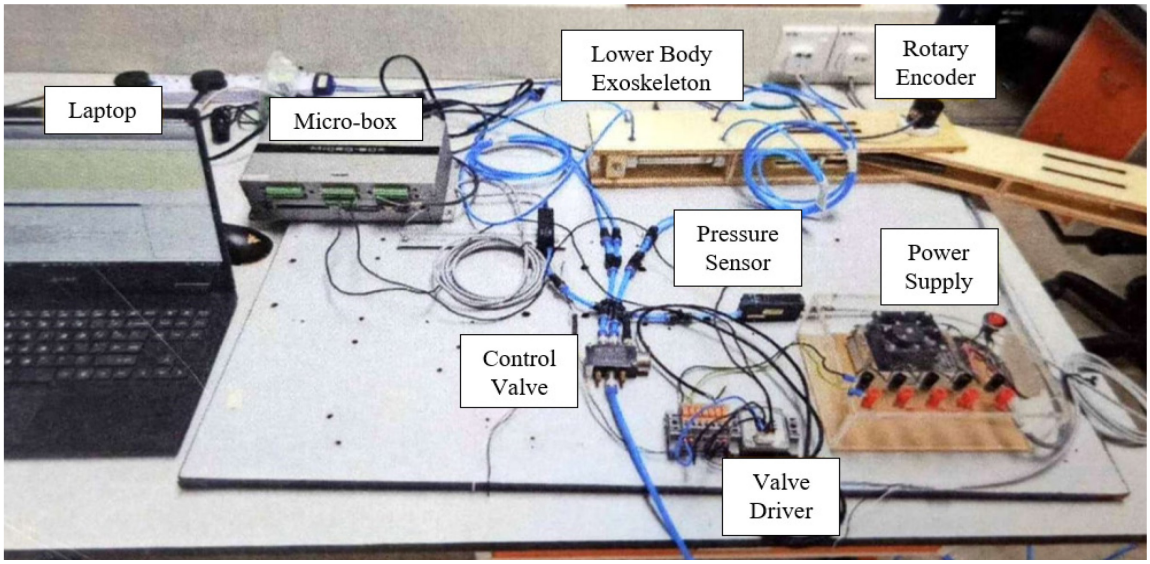

Figure 4. Overall experiment setup for the LBE system

https://doi.org/10.31436/iiumej.v25i2.3250

2.2 Characterization Of The Lower Body Exoskeleton (LBE)

The studies in this research were conducted within the operational working range of the Lower Body Exoskeleton (LBE) that is between 0° to 75° angular movement. To characterize the LBE system, the open-loop control system experiment was executed to evaluate the behavior of the LBE system. Figure 5 shows the angular motion of the LBE system to several step input voltages from 0V to 10V, under both without load and with load conditions. The displacement with load refers to the angular motion of the LBE system when a user wears the LBE device, which is equivalent to the estimated applied force of a human leg, 367 N. The LBE design had previously been verified to withstand 367N load using FEA analysis in the previous subsection. The displacement without load evaluation means that the LBE system is evaluated independently. From Figure 5, the retraction motion by the double-acting cylinder was observed below the 5V input signal, while extension motion was observed between 5-10V for both loads and without load. The findings support the hypothesis from the FEA result that the system was able to cause leg movement in the presence of an external load, though to a reduced extent. The relationship between the input voltages and the respective pressures is shown in Figure 6. The results depicted that the LBE system exhibits non-linear behaviors due to the implementation of the pneumatic cylinders. However, it does not significantly affect LBE performance. The results of this experiment demonstrate that the LBE effectively aids in leg movement. Additionally, the Finite Element Analysis (FEA) analysis confirms the functionality of the LBE prototype.

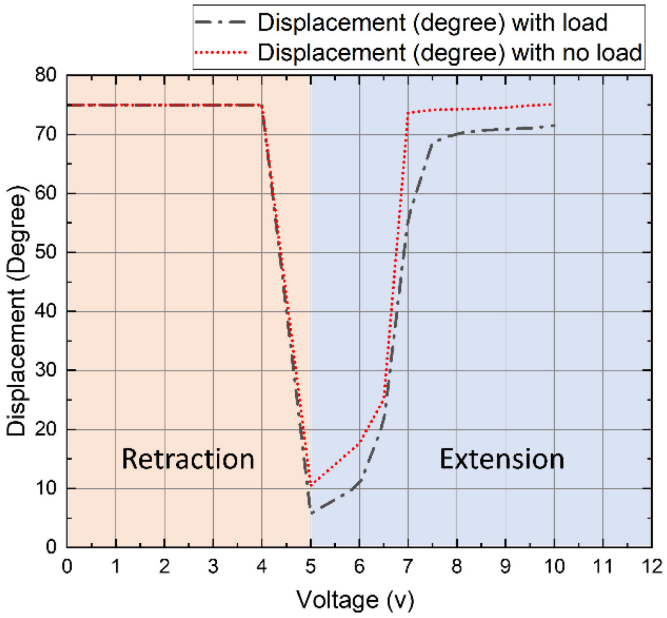

Figure 5. Angular motion of LBE with respect to several input voltages

2.3 Uncompensated Control System For The Lower Body Exoskeleton (LBE)

In order to validate the effectiveness of the Lower Body Exoskeleton (LBE) for knee rehabilitation, initially, a close-loop uncompensated control was designed, whereby a negative feedback loop was introduced, as shown in Figure 7. Figure 8 shows the testing & validation of the LBE prototype implemented, which was conducted at 45° and 75° reference, respectively. Figure 9, Table 2, and Table 3 show the results for the close-loop uncompensated, whereby the experiments were conducted with three (3) times repeatability, the results were averaged, and the standard deviation was calculated to ensure the data was reliable with low standard deviation.

https://doi.org/10.31436/iiumej.v25i2.3250

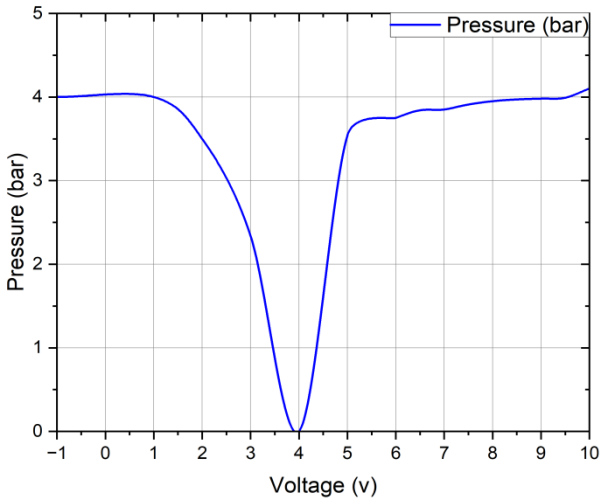

Figure 6. Non-linear characteristic of the double-acting pneumatic cylinder

It can be depicted that the LBE system shows the inability to reach the reference set point at 45° and 75°, with a high error rate, E_{ss} of 5.26° and 4.87°, respectively. It can also be observed in Tables 2 and 3 that the uncompensated control system exhibits high rise time, Tr and settling times, and T_s for the two (2) references, with relatively small overshoot values that do not significantly impact stability.

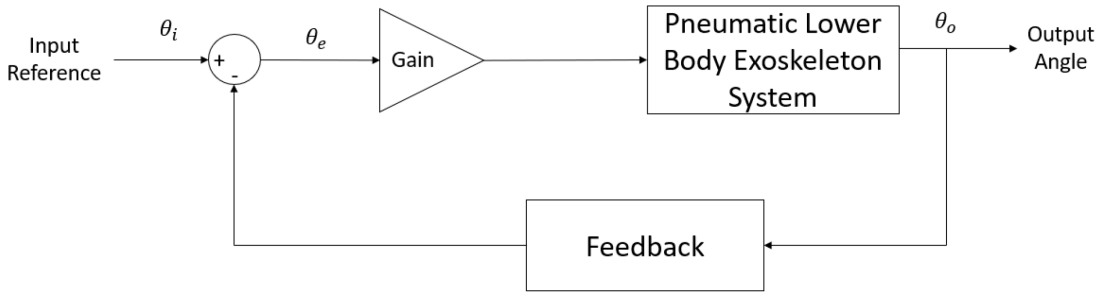

Figure 7. Close-loop uncompensated block diagram for LBE

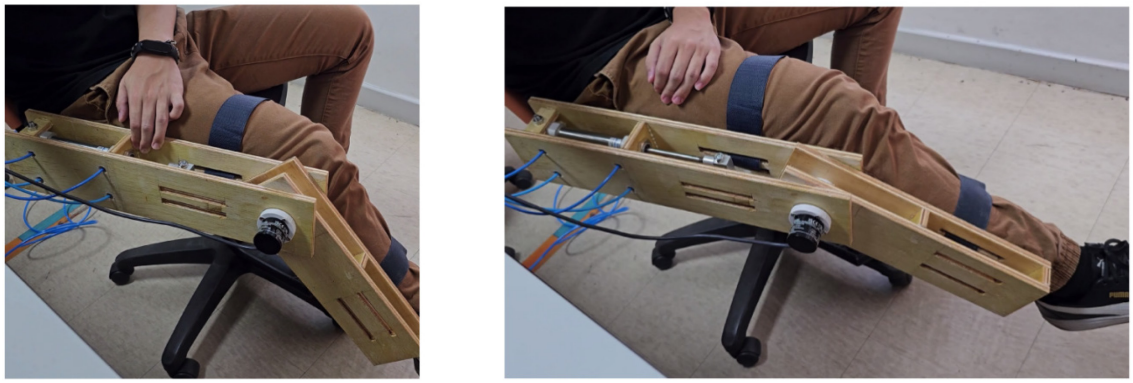

(a) Reference set point at 45° (b) Reference set point at 75°

Figure 8. Testing and validation of the LBE prototype

https://doi.org/10.31436/iiumej.v25i2.3250

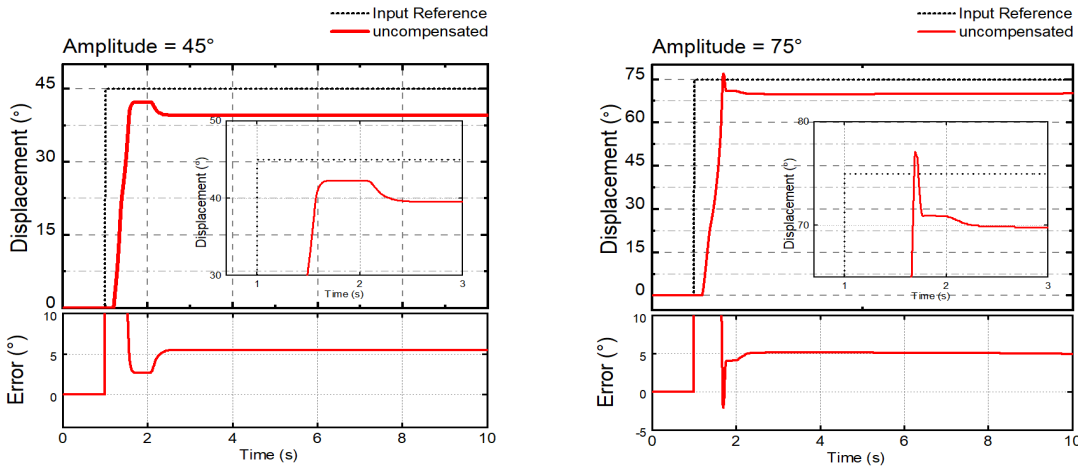

(a) Reference 45° (b) Reference 75°

Figure 9. Comparative transient parameters result for the uncompensated controller.

Table 2. The control performances of the uncompensated closed-loop controller at 45°.

System Response	Experiment			Average	Standard Deviation
	Rep 1	Rep 2	Rep 3		
Rise Time, T_r (ms)	293.0	292.1	295.3	293.5	0.00769
Settling Time, T_s (ms)	2238.1	2321.7	2227.3	2262.4	0.04103
Overshoot, OS (%)	6.9663	7.012	6.9742	6.9848	0.00817
Steady State Error, E_{ss} (°)	5.4677	5.3452	4.9789	5.2639	0.29315

Table 3. The control performances of the uncompensated closed-loop controller at 75°.

System Response	Experiment			Average	Standard Deviation
	Rep 1	Rep 2	Rep 3		
Rise Time, T_r (ms)	395.3	399.8	388.4	394.5	0.00832
Settling Time, T_s (ms)	1752.2	178.33	1728.9	1754.5	0.02693
Overshoot, OS (%)	10.0127	9.991	10.342	10.1159	0.09101
Steady State Error, E_{ss} (°)	5.09	4.52	5.01	4.8733	0.16635

2.4 Proportional Integral Derivative (PID) Controller for the LBE system

To improve the control performance, the Proportional Integral Derivative (PID) controller scheme was proposed and implemented in the LBE system, as shown in Figure 10, to reduce the rise time, settling time, percentage overshoot, and error based on the previous result. In this work, the heuristic method, i.e., trial and error method, was chosen for its practicality due to the highly non-linear behavior of the system, which was verified in the open-loop characterization. Despite being a simpler form of optimization, it allows for effective tuning of the PID controller to achieve the desired performance. The iterative nature of this method means that it inherently seeks to optimize the gain values by continuously refining them based on observed system behavior. The tuning of the PID gain was executed by initially setting the proportional parameter, K_p, and gradually increasing it from zero value until the system exhibited steady-state output. This phase determined the desired rise time, and this K_p value was then selected as the optimized value. In order to reduce the error, while maintaining K_p and K_d, which were set at zero value, the integral parameter, Ki, was then

https://doi.org/10.31436/iiumej.v25i2.3250

tuned. Fine-tuning K_i effectively eliminated system errors and enhanced the control accuracy. Finally, the derivative parameter, K_d, was tuned to enhance transient response and reduce high overshoot. The optimized PID gain for the LBE system is shown in Table 4. Tables 5 and 6 show the control performances for the PID controller scheme at 45° and 75° reference, respectively. Table 5 represents the control performances at reference 45°; the standard deviation values for parameters, i.e., rise time (T_r), settling time (T_s), overshoot, and steady-state error (E_{ss}), are low, indicating consistent and reliable results across the repeated experiments. This consistency is crucial in experimental settings as it ensures that the data obtained is reliable and the system's behavior is accurately captured. Similarly, Table 6, which shows the control performances at reference 75°, also exhibits small standard deviation values for the measured parameters. This consistency in the results at different reference angles reinforces the repeatability and reliability of the experiments with the PID gain parameters, demonstrating the controller's robustness in relation to various setpoints.

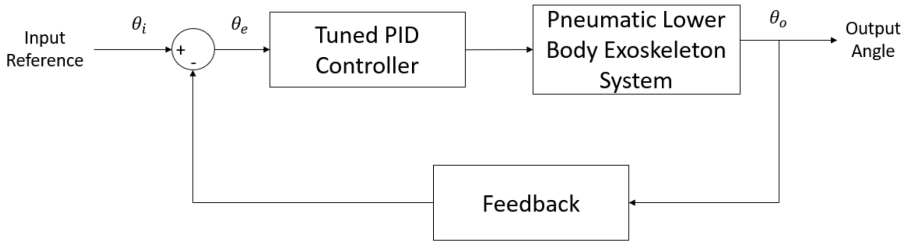

Figure 10. Close-loop block diagram with PID controller

Table 4. PID gain parameters.

PID Gain	Value
K_p	4
K_i	0.35
K_d	0.3

Table 5. The control performances of the Closed-Loop PID Controller at 45°

System Response	Experiment			Average	Standard Deviation
	Rep 1	Rep 2	Rep 3		
Rise Time, T_r (ms)	329.6	339.6	333.6	0.3343	0.00422
Settling Time, T_s (ms)	3485.9	306.79	2968.9	3.1742	0.2302
Overshoot, OS (%)	2.3669	2.56	2.56	2.4976	0.0887
Steady State Error, E_{ss} (°)	-0.04	-0.04	-0.04	-0.04	0

Table 6. The control performances of the Closed-Loop PID Controller at 75°

System Response	Experiment			Average	Standard Deviation
	Rep 1	Rep 2	Rep 3		
Rise Time, T_r (ms)	379.4	384.8	381.8	0.3819	0.00222
Settling Time, T_s (ms)	1747.1	1763.1	1753.1	1.7544	0.00702
Overshoot, OS (%)	0.1195	0.5967	0.3584	0.3582	0.2254
Steady State Error, E_{ss} (°)	0.5549	0.1107	0.3772	0.3476	0.2149

https://doi.org/10.31436/iiumej.v25i2.3250

3. RESULTS AND DISCUSSION

This section will discuss and compare the effectiveness of the closed-loop PID controller to the uncompensated system. Tables 7 and 8 discussed the comparative analysis of transient parameters for both the uncompensated closed-loop system and the PID controller at reference angles of 45° and 75°, respectively. Concurrently, the comparative result is visually represented in Figure 11. At reference 45°, the PID controller showed an improvement in rise time, Tr, by 40.8ms, equivalent to 13.9% compared to the uncompensated system, as well as a significant improvement by 911.8ms in the settling time, Ts, i.e., 40.3% improvement. Additionally, there was a distinct reduction in percentage overshoot, OS% by 4.4872%, signifying a substantial 64.26% decrease and a 5.2639° reduction in steady-state error, E_{ss} achieving a complete 100% reduction at the 45° reference angle. The increased rise time, T_r, and settling time, Ts, in this context can be attributed to the unique challenges posed by small reference angles and the non-linear behavior of the LBE system, as mentioned in Section 2. In such scenarios, the control system must meticulously fine-tune its responses to reach the desired setpoint. At the 75° reference, the PID controller demonstrates notable improvements, with a 3.2% reduction in rise time, $T_{r,}$ and a mere 0.006% change in settling time, T_s. Moreover, there is a substantial 96.5% decrease in overshoot, OS%, and a remarkable 92.9% reduction in steady-state error, E_{ss}. In summary, the proposed PID controller significantly enhanced the performance of the LBE system, as the analysis of the system's response to reference angles of 45° and 75° revealed substantial improvements in various key performance parameters.

Table 7. Controller performance comparison at reference 45°

Parameters		**Reference 45^0**		
		Uncompensated	**PID**	**Improvement (%)**
Overshoot, OS (%)	**Average**	6.9848	2.4976	64.26%
	Standard Deviation	0.00817	0.00887	
Steady State Error, E_{ss} (^{o})	**Average**	5.2639	0	100%
	Standard Deviation	0.29315	0	
Rise Time, T_r (ms)	**Average**	293.5	334.3	13.9%
	Standard Deviation	7.69	4.22	
Settling Time, T_s (ms)	**Average**	2262.4	3174.2	40.3%
	Standard Deviation	41.03	230.2	

https://doi.org/10.31436/iiumej.v25i2.3250

Table 8. Controller performance comparison at reference 75°

Parameters		Reference 75^0		
		Uncompensated	PID	Improvement (%)
Overshoot, OS (%)	**Average**	10.1159	0.3582	96.5%
	Standard Deviation	0.09101	0.2254	
Steady State Error, E_{ss} (°)	**Average**	4.8733	0.3476	92.9%
	Standard Deviation	0.16635	0.2149	
Rise Time, T_r (ms)	**Average**	394.5	381.9	3.2%
	Standard Deviation	8.32	2.22	
Settling Time, T_s (ms)	**Average**	1754.5	1754.4	0.006%
	Standard Deviation	26.93	7.02	

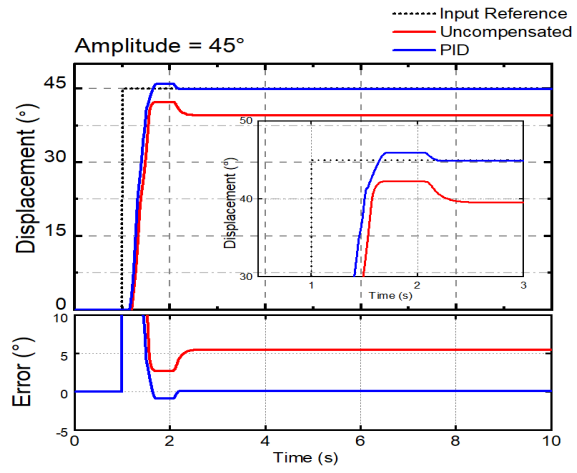

(a) Reference 45°

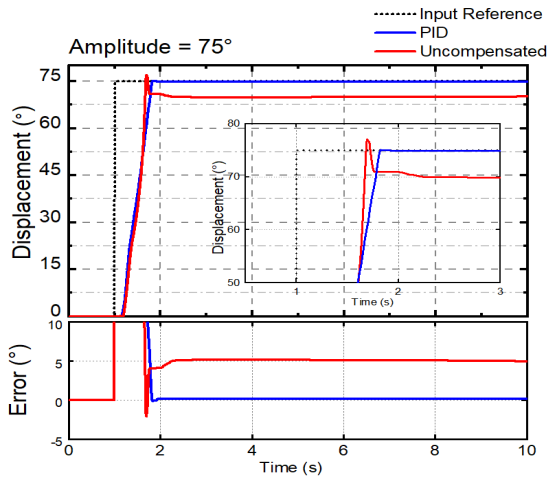

(a) Reference 75°

Figure 11. Comparative transient parameters result in uncompensated and PID controller

4. CONCLUSION

In summary, this research successfully achieved its main objective, which was to design a motion controller for a lightweight lower body exoskeleton (LBE) using a slider-crank mechanism dedicated to knee joint rehabilitation. The lower body exoskeleton (LBE) prototype was developed by first implementing the Finite Element Analysis (FEA) method to optimize the design parameters, ensuring the reliability of the prototype. The characteristics of the LBE prototype were then evaluated to confirm the non-linear behavior of the LBE system due to the implementation of the pneumatic double-acting cylinders. The system was then further evaluated using a PID controller to analyze the control performances. The PID closed-loop system exhibited excellent control performances, whereby at reference 45°, the controller showed an improvement in terms of reduction of the overshoot, OS% by 64.26%, and an impressive decrease in steady-state error, E_{ss} by 100% even though there was an increased in rise time, T_r and settling time, T_s. At the 75° reference angle, there was an improvement in rise time, T_r, and settling time; Ts were a substantial 96.5% reduction in

overshoot, OS% accompanied by a significant 92.9% decrease in steady-state error, E_{ss}. These findings depicted the PID controller's efficacy in achieving faster response times, enhancing stability, minimizing overshoot, and greatly improving accuracy and precision in maintaining desired reference angles. Potential future research may aim to enhance the extent of movement and modify the exoskeleton to accommodate bilateral leg utilization. By integrating motion and torque analysis, as well as finite element analysis, the optimization of gait training can be enhanced while also guaranteeing the exoskeleton's safety and durability. These areas of research have the potential to advance the field of lower body exoskeletons for rehabilitation and provide additional benefits to people undergoing rehabilitation.

ACKNOWLEDGEMENT

The authors wish to express their gratitude to Motion Control Research Laboratory (MCon Lab), Center for Robotics and Industrial Automation (CeRIA), Centre for Research and Innovation Management (CRIM), Fakulti Teknologi dan Kejuruteraan Elektrik (FTKE), and Universiti Teknikal Malaysia Melaka (UTeM) for supporting this research and publication.

REFERENCES

[1] Pamungkas DS, Caesarendra W, Soebakti H, Analia R, Susanto S. (2019) Overview: Types of Lower Limb Exoskeletons. Electronics, 8(11): 1283. doi: 10.3390/electronics8111283.

[2] Wu Q, Wang X, Du F, Zhang X. (2015) Design and control of a powered hip exoskeleton for walking assistance. International Journal of Advanced Robotic Systems, 12(3): 18. doi: 10.5772/59757.

[3] Yeem S, Heo J, Kim H, Kwon Y. (2019) Technical analysis of exoskeleton robot. World Journal of Engineering and Technology, 7:68–79. http://dx.doi.org/10.4236/wjet.2019.71004.

[4] Tang X, Wang X, Ji X, Zhou Y, Yang J, Wei Y, Zhang W. (2022) A Wearable Lower Limb Exoskeleton: Reducing the Energy Cost of Human Movement. Micromachines, 13:900. doi: 10.3390/mi13060900.

[5] Rupal BS, Rafique S, Singla A, Singla E, Isaksson M, Virk GS. (2017) Lower-limb exoskeletons: Research trends and regulatory guidelines in medical and non-medical applications. International Journal of Advanced Robotic Systems, 14(6):172988141774355. doi:10.1177/1729881417743554.

[6] Karis MS, Kasdirin HA, Abas N, Saad WHM, Aras MSM. (2023) Emg based control of wrist exoskeleton. IIUM Engineering Journal, 24:391–406. doi: 10.31436/iiumej.v24i2.2804.

[7] Sharma CAA, Sai VKASK, Prasad A, Begum R, Sharvani GS, Manjunath AE. (2018) Multifaceted bio-medical applications of exoskeleton: A review. 2018 2nd International Conference on Inventive Systems and Control (ICISC). doi: 10.1109/icisc.2018.8399053.

[8] Song G, Huang R, Qiu J, Cheng H, Fan S. (2020) Model-based control with interaction predicting for human-coupled lower exoskeleton systems. Journal of Intelligent & Robotic Systems, 100:389–400. doi: 10.1007/s10846-020-01200-5.

[9] Tanaka T, Matsumura R, Miura T. (2022) Influence of varied load assistance with exoskeleton-type robotic device on gait rehabilitation in healthy adult men. International Journal of Environmental Research and Public Health, 19:9713. doi: 10.3390/ijerph19159713.

[10] Van DF, Hesse N, Labruyère R. (2023) Markerless motion tracking to quantify behavioural changes during robot-assisted gait training: A validation study. Frontiers in Robotics and AI, 10. doi: 10.3389/frobt.2023.1155542.

[11] Van NIJ, Van DRB, Van HFH, Rijken H, Geurts AC, Keijsers NL. (2022) Improvement of quality of life after 2-month exoskeleton training in patients with chronic spinal cord injury. The Journal of Spinal Cord Medicine, 47(3): 354–360. doi: 10.1080/10790268.2022.2052502.

[12] Gomez VD, Ballen MF, Rodriguez GC, Munera M, Cifuentes CA. (2021) Experimental characterization of the T-FLEX ankle exoskeleton for gait assistance. Mechatronics, 78: 102608. https://doi.org/10.1016/j.mechatronics.2021.102608.

[13] Masengo G, Zhang X, Dong R, Alhassan AB, Hamza K, Mudaheranwa E. (2023) Lower limb exoskeleton robot and its cooperative control: A review, trends, and challenges for future research. Frontiers in Neurorobotics, 16. doi: 10.3389/fnbot.2022.913748.

[14] Shi D, Zhang W, Zhang W, Ding X. (2019) A Review on lower limb rehabilitation exoskeleton robots. Chinese Journal of Mechanical Engineering, 32(1). doi: 10.1186/s10033-019-0389-8.

[15] Ren B, Luo X, Li H, Chen, J, Wang Y. (2021) Gait trajectory-based interactive controller for lower limb exoskeletons for construction workers. Computer-Aided Civil and Infrastructure Engineering, 37(5): 558–572. doi: 10.1111/mice.12756.

[16] Pina D, Gabriel J, Natal R (2019) Motion capture and multibody simulations to determine actuation requirements for an assistive exoskeleton. Proceedings of the 12th International Joint Conference on Biomedical Engineering Systems and Technologies. doi: 10.5220/0007403601830191.

[17] Gong H, Song Z, Dario P. (2021) Design of a novel wheelchair-exoskeleton robot for human multi-mobility assist. Intelligent Robotics and Applications: 281–292. doi: 10.1007/978-3-030-89134-3_26.

[18] Foroutannia A, Akbarzadeh TMR, Akbarzadeh A, Tahamipour ZSM. (2023) Adaptive fuzzy impedance control of exoskeleton robots with electromyography-based convolutional neural networks for human intended trajectory estimation. Mechatronics, 91: 102952. doi: 10.1016/j.mechatronics.2023.102952.

[19] Ali SA, Annuar KAM, Miskon MF. (2016) Trajectory planning for exoskeleton robot by using cubic and quintic polynomial equation. International Journal of Applied Engineering Research, 11(13): 7943-7946.

[20] Wu Q, Wang X, Du F, Zhang X. (2015) Design and control of a powered hip exoskeleton for walking assistance. International Journal of Advanced Robotic Systems, 12(3): 18. doi: 10.5772/59757.

[21] Yeem S, Heo J, Kim H, Kwon Y. (2019) Technical analysis of exoskeleton robot. World Journal of Engineering and Technology, 07(01): 68–79. doi: 10.4236/wjet.2019.71004.

[22] Chen G, Chan CK, Guo Z, Yu H. (2013) A review of lower extremity assistive robotic exoskeletons in rehabilitation therapy. Critical Reviews in Biomedical Engineering, 41(4–5): 343–363. doi: 10.1615/critrevbiomedeng.2014010453.

[23] Rupal BS, Rafique S, Singla A, Singla E, Isaksson M, Virk GS. (2017) Lower-limb exoskeletons. International Journal of Advanced Robotic Systems, 14(6): 172988141774355. doi: 10.1177/1729881417743554.

[24] Yuden MMA, Ghazaly MM, Amran AC, Jamaludin IW, Khoo HY, Yaacob MR, Abdullah Z, Yeo CK. (2016) Positioning control performances of a robotic hand system. Jurnal Teknologi, 79(1). doi: 10.11113/jt.v79.8726.

[25] Miao Y, Gao F, Pan D. (2013) Mechanical design of a hybrid leg exoskeleton to augment load-carrying for walking. International Journal of Advanced Robotic Systems, 10(11): 395. doi: 10.5772/57238.

[26] Guo Z, Yu H, Yin YH (2014) Developing a mobile lower limb robotic exoskeleton for gait rehabilitation. Journal of Medical Devices, 8(4). doi: 10.1115/1.4026900.

[27] Luu TP, Low KH, Qu X, Lim HB, Hoon KH. (2014) Hardware development and locomotion control strategy for an over-ground gait trainer: NaTUre-Gaits. IEEE Journal of Translational Engineering in Health and Medicine, 2: 1–9. doi: 10.1109/jtehm.2014.2303807.

[28] Yves S, Bouri M, Clavel R, Allemand Y, Brodard R. (2010) A novel verticalized reeducation device for spinal cord injuries: the walktrainer, from design to clinical trials. Robotics 2010 Current and Future Challenges. doi: 10.5772/7328.

[29] Stearns YKA, Brenner LA. (2018) Novel psychological outcomes with ekso bionics technology. Archives of Physical Medicine and Rehabilitation, 99(10). doi: 10.1016/j.apmr.2018.07.249.

[30] Strausser KA, Swift TA, Zoss AB, Kazerooni H, Bennett BC. (2011) Mobile exoskeleton for spinal cord injury: development and testing. ASME 2011 Dynamic Systems and Control Conference and Bath/ASME Symposium on Fluid Power and Motion Control, 2. doi:

10.1115/dscc2011-6042.

[31] Jyräkoski T, Merilampi S, Puustinen J, Kärki A. (2021) Over-ground robotic lower limb exoskeleton in neurological gait rehabilitation: User experiences and effects on walking ability. Technology and Disability, 33(1): 53–63. doi: 10.3233/tad-200284.

[32] Baronchelli F, Zucchella C, Serrao M, Intiso D, Bartolo M. (2021) The effect of robotic assisted gait training with lokomat® on balance control after stroke: systematic review and meta-analysis. Frontiers in Neurology, 12. doi: 10.3389/fneur.2021.661815.

[33] Ruffaldi E, Barsotti M, Leonardis D, Bassani G, Frisoli A, Bergamasco M. (2014) Evaluating virtual embodiment with the alex exoskeleton. Haptics: Neuroscience, Devices, Modeling, and Applications: 133–140. doi: 10.1007/978-3-662-44193-0_18.

[34] Sapiee MR, Marhaban MHM, Miskon MF, Ishak AJ (2020) Walking simulation model of lower limb exoskeleton robot design. Journal of Mechanical Engineering and Sciences, 14(3): 7071–7081. doi: 10.15282/jmes.14.3.2020.09.0554.

[35] Bogue R. (2017). Robots that interact with humans: a review of safety technologies and standards. Industrial Robot: An International Journal, 44(4): 395–400. doi: 10.1108/ir-04-2017-0070.

[36] Ward D, Epstein B, Tiziani L, Hammond FL. (2021) Optimal design of a mechatronic lever arm for pneumatic exoskeleton: design and validation. 2021 Design of Medical Devices Conference. doi: 10.1115/dmd2021-1093.

[37] Zoss A, Kazerooni H, Chu A. (2005) On the mechanical design of the Berkeley Lower Extremity Exoskeleton (BLEEX). 2005 IEEE/RSJ International Conference on Intelligent Robots and Systems. doi: 10.1109/iros.2005.1545453.

[38] Li Y, Guan X, Han X, Tang Z, Meng K, Shi Z, Penzlin B, Yang Y, Ren J, Yang Z, Li Z, Leonhardt S, Ji L. (2020) Design and preliminary validation of a lower limb exoskeleton with compact and modular actuation. IEEE Access, 8: 66338–66352. doi: 10.1109/access.2020.2985910.

[39] Lee H, Ferguson PW, Rosen J. (2020) Lower limb exoskeleton systems—overview. wearable robotics: 207–229. doi: 10.1016/b978-0-12-814659-0.00011-4.

[40] Song J, Zhu A, Tu Y, Zhang X, Cao G. (2023) Novel Design and control of a crank-slider series elastic actuated knee exoskeleton for compliant human–robot interaction. IEEE/ASME Transactions on Mechatronics, 28(1): 531–542. doi: 10.1109/tmech.2022.3204921.

[41] Shao Y, Zhang W, Su Y, Ding X. (2021) Design and optimisation of load-adaptive actuator with variable stiffness for compact ankle exoskeleton. Mechanism and Machine Theory, 161: 104323. doi: 10.1016/j.mechmachtheory.2021.104323.

[42] Brisson N, Krämer M, Reichenbach J, Duda G. (2021) Dynamic and guided knee motion under loading during fast magnetic resonance imaging: a novel device. Osteoarthritis and Cartilage, 29: S350–S351. doi: 10.1016/j.joca.2021.02.455.

[43] Miura T, Matsubara A, Kono D, Otaka K, Hoshide K. (2017) Design of high-precision ball screw based on small-ball concept. Precision Engineering, 47: 452–458. doi: 10.1016/j.precisioneng.2016.09.020.

[44] Sankai Y. (2010) HAL: Hybrid assistive limb based on cybernics. Springer Tracts in Advanced Robotics: 25–34. doi: 10.1007/978-3-642-14743-2_3.

[45] Sun Y, Hu J, Huang R. (2023) Negative-stiffness structure vibration-isolation design and impedance control for a lower limb exoskeleton robot. Actuators, 12(4): 147. doi: 10.3390/act12040147.

[46] Krause J. (2019) The Methodology of conventional arms control. Prospects for Conventional Arms Control in Europe: 28–62. doi: 10.4324/9780429303241-4.

[47] Zaway I, Jallouli KR, Maaleja B, Medhaffar H, Derbela N. (2022) Multi-objective fractional order pid controller optimization for kid's rehabilitation exoskeleton. International Journal of Robotics and Control Systems, 3(1): 32–49. doi: 10.31763/ijrcs.v3i1.840.

[48] Mathew M, Thomas MJ, Navaneeth M, Sulaiman S, Amudhan A, Sudheer A. (2022) A systematic review of technological advancements in signal sensing, actuation, control and training methods in robotic exoskeletons for rehabilitation. Industrial Robot: The International

Journal of Robotics Research and Application, 50(3): 432–455. doi: 10.1108/ir-09-2022-0239.

[49] Vantilt J, Tanghe K, Afschrift M, Bruijnes AK, Junius K, Geeroms J, Aertbeliën E, De Groote F, Lefeber D, Jonkers I, De Schutter J. (2019) Model-based control for exoskeletons with series elastic actuators evaluated on sit-to-stand movements. Journal of NeuroEngineering and Rehabilitation, 16(1). doi: 10.1186/s12984-019-0526-8.

[50] Kardan I, Akbarzadeh A. (2017) Robust output feedback assistive control of a compliantly actuated knee exoskeleton. Robotics and Autonomous Systems, 98: 15–29. doi: 10.1016/j.robot.2017.09.006.

[51] Villa PAC, Delisle RD, Botelho T, Mayor JJV, Delis AL, Carelli R, Frizera NA, Bastos TF. (2018) Control of a robotic knee exoskeleton for assistance and rehabilitation based on motion intention from sEMG. Research on Biomedical Engineering, 34(3): 198–210. doi: 10.1590/2446-4740.07417.

[52] Lenzi T, De Rossi SMM, Vitiello N, Carrozza MC. (2012) Intention-based emg control for powered exoskeletons. IEEE Transactions on Biomedical Engineering, 59(8): 2180–2190. doi: 10.1109/tbme.2012.2198821.

[53] Ling L, Wang Y, Ding F, Jin L, Feng B, Li W, Wang C, Li X. (2023) An efficient method for identifying lower limb behaviour intentions based on surface electromyography. computers, Materials & Continua, 77(3): 2771–2790. doi: 10.32604/cmc.2023.043383.

[54] De Miguel FJ, Lobo PJ, Prinsen E, Font LJM, Marchal CL. (2023) Control strategies used in lower limb exoskeletons for gait rehabilitation after brain injury: a systematic review and analysis of clinical effectiveness. Journal of NeuroEngineering and Rehabilitation, 20(1). doi: 10.1186/s12984-023-01144-5.

[55] Longatelli V, Pedrocchi A, Guanziroli E, Molteni F, Gandolla, M. (2021) Robotic exoskeleton gait training in stroke: an electromyography-based evaluation. Frontiers in Neurorobotics, 15. doi: 10.3389/fnbot.2021.733738.

[56] Adeola-Bello ZA, Azlan NZ. (2022) Power assist rehabilitation robot and motion intention estimation. International Journal of Robotics and Control Systems, 2(2): 297–316. doi: 10.31763/ijrcs.v2i2.650.

[57] Wickiewicz TL, Roy RR, Powell PL, Edgerton VR. (1983) Muscle architecture of the human lower limb. Clinical Orthopaedics and Related Research, 179: 275-283. doi: 10.1097/00003086-198310000-00042.

[58] Motl R, Gosney J. (2008) Effect of exercise training on quality of life in multiple sclerosis: a meta-analysis. Multiple Sclerosis Journal, 14(1): 129–135. doi: 10.1177/1352458507080464.